SANDIA REPORT

SAND2005-6230
Unlimited Release
Printed October 2005

Binary Electrokinetic Separation of Target DNA from Background DNA Primers

Conrad D. James and Mark Derzon

Prepared by
Sandia National Laboratories
Albuquerque, New Mexico 87185 and Livermore, California 94550

Sandia is a multiprogram laboratory operated by Sandia Corporation,
a Lockheed Martin Company, for the United States Department of Energy's
National Nuclear Security Administration under Contract DE-AC04-94AL85000.

Issued by Sandia National Laboratories, operated for the United States Department of Energy by Sandia Corporation.

Available to DOE and DOE contractors from
U.S. Department of Energy
Office of Scientific and Technical Information
P.O. Box 62
Oak Ridge, TN 37831

Telephone: (865)576-8401
Facsimile: (865)576-5728
E-Mail: reports@adonis.osti.gov
Online ordering: http://www.osti.gov/bridge

Available to the public from
U.S. Department of Commerce
National Technical Information Service
5285 Port Royal Rd
Springfield, VA 22161

Telephone: (800)553-6847
Facsimile: (703)605-6900
E-Mail: orders@ntis.fedworld.gov
Online order: http://www.ntis.gov/help/ordermethods.asp?loc=7-4-0#online

SAND2005-6230
Unlimited Release
Printed October 2005

Binary Electrokinetic Separation of Target DNA from Background DNA Primers

Conrad D. James
and Mark Derzon, MEMS Device Technologies

Sandia National Laboratories
P.O. Box 5800
Albuquerque, New Mexico 87185-1080

Abstract

This report contains the summary of LDRD project 91312, titled "Binary Electrokinetic Separation of Target DNA from Background DNA Primers".

This work is the first product of a collaboration with Columbia University and the Northeast BioDefense Center of Excellence. In conjunction with Ian Lipkin's lab, we are developing a technique to reduce false positive events, due to the detection of unhybridized reporter molecules, in a sensitive and multiplexed detection scheme for nucleic acids developed by the Lipkin lab. This is the most significant problem in the operation of their capability. As they are developing the tools for rapidly detecting the entire panel of hemorrhagic fevers this technology will immediately serve an important national need.

The goal of this work was to attempt to separate nucleic acid from a preprocessed sample. We demonstrated the preconcentration of kilobase-pair length double-stranded DNA targets, and observed little preconcentration of 60 base-pair length single-stranded DNA probes. These objectives were accomplished in microdevice formats that are compatible with larger detection systems for sample pre-processing.

Combined with Columbia's expertise, this technology would enable a unique, fast, and potentially compact method for detecting/identifying genetically-modified organisms and multiplexed rapid nucleic acid identification. Another competing approach is the DARPA funded IRIS Pharmaceutical TIGER platform which requires many hours for operation, and an 800k$ piece of equipment that fills a room. The Columbia/SNL system could provide a result in 30 minutes, at the cost of a few thousand dollars for the platform, and would be the size of a shoebox or smaller.

Acknowledgements

We would like to thank all of the people who were instrumental in this project, specifically our collaborators W. Ian Lipkin, Gustavo Palacios, and Omar Jabado (Columbia University) as well as Dave Norwood, and George Ludwig of USAMRIID. We also extend our gratitude to the Microelectronics Development Laboratory for fabrication of the silicon microfluidic devices, and to Jeb Flemming and Darren Branch for the glass substrate devices fabricated at the Compound Semiconductor Research Laboratory. Sandia is a multiprogram laboratory operated by Sandia Corporation, a Lockheed Martin Company, for the United States Department of Energy under contract DE-ACO4-94-AL85000.

Contents

Figures

Nomenclature

AC	alternating current
bp	base-pair
DEP	dielectrophoresis
DNA	deoxyribonucleic acid
dsDNA	double-stranded DNA
kbp	kilobase-pair
pDEP	positive dielectrophoresis
RF	radio frequency
nDEP	negative dielectrophoresis
SNL	Sandia National Laboratories
ssDNA	single-stranded DNA
SwIFT™	Surface Micromachining with Integrated Fluidic Technology

1.0 Introduction

W. Ian Lipkin's lab was the first to identify the West Nile virus, and more recently, the SARS virus. They found these organisms using the digital strand diagnostic display (DSDD) technique that they pioneered; this is a broadband polymerase chain reaction (PCR). In addition, they recently created a panel of assays for the list of hemorrhagic fevers using their unique mass tag technology and they are combining them. During a recent Northeast Center of Excellence in BioDefense meeting, after Mark Derzon presented work on the SNL/USAMRIID diagnostic development effort, Ian Lipkin's group requested assistance specifically to employ SNL technology to reduce the false positive rate in their detection methodology.

After discussion, we determined that modifications to the existing Sandia microfluidics technology developed in a previous LDRD (SAND2004-5465) could potentially remove low-mass PCR hybridization components that result in false positive detections. Combining this capability with Columbia's expertise would enable a unique, fast, and potentially compact method for detecting/identifying genetically-modified organisms and multiplexed (many pathogen) rapid nucleic acid identification. The only competing approach is the DARPA-funded IRIS Pharmaceutical TIGER platform which requires many hours of operation, and an 800k$ piece of equipment that fills a room. The Columbia/SNL system could provide a result in 30 minutes, at the cost of a few $k for the platform and a few dollars per test (in production), and would be the size of a shoebox or smaller.

The LDRD funds were to allow us to show the ability to trap and sequester nucleic acids of appropriate mass. This allowed us determine whether or not the device could separate or 'clean up' the samples as provided by Columbia. It was known in advance that this would only provide a 'proof-of-principle' for separation and the resources would not be adequate to complete proof of false positive reduction; that will be performed at a later date. Sandia's expertise in microfabrication and electrokinetic assays makes this a unique opportunity for contributing to the Northeast Center of Excellence in which we are partnered with Columbia University.

Clearly the need to process samples and assist Columbia and the Northeast BioDefense Center of excellence is worthwhile in its own right. Secondary considerations for performing this work are also worth mentioning. We gained experience handling the nucleic acid on the same platform and materials that we are using for the bead based work being performed to meet the Joint Program Executive Offices Block III biodefense countermeasures needs and as such we plan to use the new information as proof-of-principle results in other projects with both Columbia and USAMRIID.

The difficulty encountered with the PCR technique developed at Columbia University is the occurrence of false positives. The technique involves hybridizing a single-stranded DNA (ssDNA) reporter oligonucleotide (~ 50 bp) to a target double-stranded DNA

(dsDNA) molecule (>1000 bp) for subsequent amplification. The ssDNA reporter binds to a ss tail of the dsDNA target. The road-block for this work lies in the fact that unhybridized reporter oligonucleotides need to separated from hybridized target-reporter molecules, as the unhybridized oligonucleotides produce false positives in the detector.

The testing performed during the LDRD using SNL's electrokinetic separation technology appears to provide a solution in that the appropriate sized nucleic acids are trapped and then released.

2.0 Dielectrophoresis of DNA Molecules

Our previous SAND report details the general phenomenon of dielectrophoresis (DEP) for particles (SAND2004-5465). Here, we will consider the more complicated phenomenon of DEP of small polyelectrolytes such as DNA, a phenomenon that has been studied by numerous labs [1-5]. We consider a DNA molecule suspended in a fluid with permittivity ε_f and conductivity σ_f [Figure 1]. DNA molecules are negatively charged due to the phosphate group on each nucleotide. These negative charges are shielded by a counterion cloud, producing charge neutrality for the molecule. Under an electric field, the mobile counterion cloud is distorted, and produces a net charge density σ_m along the length of the molecule [6]. In addition, the polarization (a relative shift of positive and negative electric charges) of the cloud produces a net dipole moment **p**. Both the charge and the dipole moment lead to DEP of DNA. This DEP phenomenon is postulated to occur with electric fields at low frequencies (~10 kHz).

At higher frequencies (MHz), the DEP phenomenon observed with DNA molecules has not been well explained, as the mobility of the counterion cloud at these frequencies is not well understood. The conventional analysis of high frequency DEP for micron sized particles has utilized the Maxwell-Wagner effect [7]. In the case where a particle and fluid have different permittivities and conductivities, charge will build up at the interface between the particle and the fluid. A polarized particle subject to a spatially non-uniform

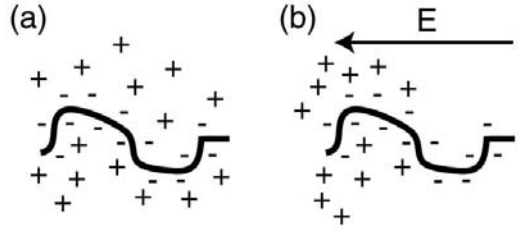

Figure 1: (a) DNA molecule with its negatively charged backbone surrounded by a counterion cloud. (b) Under an electric field, the counterion cloud becomes polarized.

electric field experiences a DEP force. The time averaged dielectrophoretic force in an AC field, F_{DEP}, is proportional to the product of the particle volume, v_p, the gradient of the square of the rms (root mean average) of the field strength, and the real component of the relative particle polarization, $\beta^*(\omega)$, at the field frequency ω:

$$\boldsymbol{F}_{DEP} = \frac{3}{2}\varepsilon_0 \varepsilon_f v_p \,\mathrm{Re}\left(\beta^*(\omega)\right)\nabla E_{rms}^2$$

$$\text{with } \beta^*(\omega) = \frac{\varepsilon_p^{\,*} - \varepsilon_f^{\,*}}{\varepsilon_p^{\,*} + 2\varepsilon_f^{\,*}} \text{ and } \varepsilon^* = \varepsilon - j\frac{\sigma}{\omega} \qquad \text{Eq. 1}$$

where ε_0 is the vacuum permittivity, $\sigma_{p/f}$ is the particle/fluid conductivity, $\varepsilon^*_{p/f}$ is the complex permittivity of the particle/fluid. The electric field must be non-uniform ($\nabla E^2_{rms} \neq 0$), and a discontinuity in ε^* between the particle and the fluid must exist in order for particle motion to occur. The gradient in the electric field leads to a nonsymmetrical dipole in the particle. This produces a net force on the particle accompanied by motion. If the particle is more polarizable than the liquid ($\mathrm{Re}(\beta^*) > 0$), the particle will migrate towards regions of maximum ∇E^2_{rms}, termed positive dielectrophoresis (pDEP). If the particle is less polarizable than the fluid ($\mathrm{Re}(\beta^*) < 0$), the particle will migrate towards regions of low ∇E^2_{rms}, termed negative dielectrophoresis (nDEP). The major benefit of using MHz frequencies is the elimination of electrochemistry, specifically, the electrolysis of water which leads to gas bubble production that will clog microfluidic devices. In addition, we can also eliminate low frequency effects (electrophoresis and electroosmosis) and use larger voltage amplitudes (20 V p-p).

To apply this analysis to DNA molecules, several points must be considered. The relative particle polarization, $\beta^*(\omega)$, only applies to spherical particles, and it has been observed that DNA undergoing DEP is stretched into an ellipsoid [8]. So in the case of an ellipsoid with major axis a and minor axis b, we have:

$$\beta^*(\omega) = \frac{\varepsilon_p^{\,*} - \varepsilon_f^{\,*}}{3[A(\varepsilon_p^{\,*} - \varepsilon_f^{\,*}) + \varepsilon_m^{\,*}]}$$

$$\text{where } A = \frac{1-e^2}{2e^3}\left[\log\left(\frac{1+e}{1-e}\right) - 2e\right],\ e = \sqrt{1-\left(\frac{b}{a}\right)^2} \qquad \text{Eq. 2}$$

In the case of DNA (as with particles), the total conductivity of DNA is given by $\sigma_p = \sigma_b - 2K_s/b$. This analysis by Zheng et al. is the most exhaustive for DEP of DNA, but there are some discrepancies that are left to be addressed. The DEP effect on DNA is only observed in low-conductivity solutions (<mS/cm), indicating the influence of the counterion cloud (a lower conductivity solution leads to a thicker Debye length, and thus a larger volume counterion cloud surrounding the molecule). An added benefit of low conductivity buffer is the reduction in Joule heating upon application of the electric field ($J=\sigma E^2$). A final consideration is that for small molecules, the DEP force is significantly opposed by the thermal energy of the molecule (kT), where k is the Boltzman constant and T is the temperature. The ratio of the DEP force to the Brownian motion force is

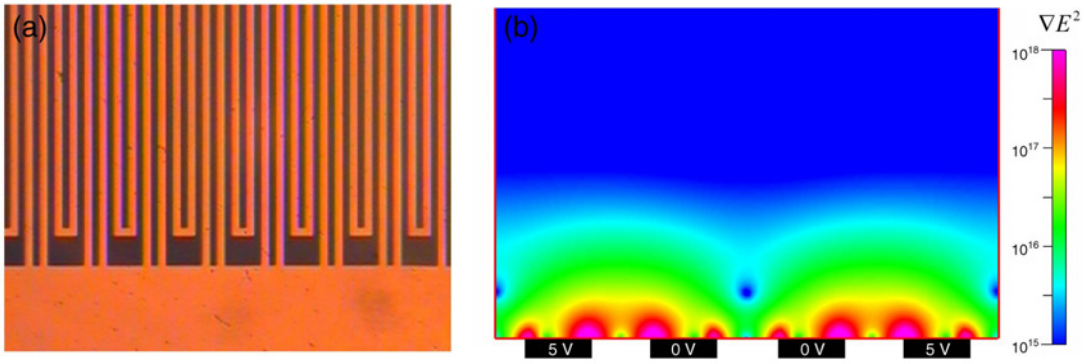

Figure 2: (a) Interdigitated (IDT) comb microelectrode device. The double-pronged microelectrodes are 5 μm wide with 5 μm spaces. (b) Cross-section image of the simulated ∇E^2 produced from the IDT device.

proportional to the radius of the particle to the fourth power [8]. Thus larger field gradients are usually required to overcome Brownian motion of small molecules. Surface micromachined devices are advantageous for this purpose, as photolithography can produce feature sizes on the order of 1 μm. This produces large electric field gradients ($\nabla E \sim 10^{13}$ V/m^2), and thus large DEP forces ($F_{DEP} \propto E\nabla E$). Our lab has previously demonstrated micro-scale separation of bacteria and polymer microspheres using DEP and an accompanying field-induced phase separation [9,10]. Some of the disadvantages of this technique are the dependence of the polarization effect on the buffer (low ionic strength solutions are needed for trapping DNA) and the unknown effects that the strong electric field will have on the integrity of the DNA molecule.

Our primary contention for this work is that the size disparity between the dsDNA targets and ssDNA probes is sufficient for using DEP for separation. A bp is approximately 0.3 nm in length (and approximately 660 daltons in weight) meaning that a 50 bp oligo is ~ 15 nm in length and a 1000 bp molecule will be ~300 nm in length. Austin et al. demonstrated a difference of a factor of ~2 for the DEP force on a ssDNA and dsDNA molecule of the same length, and argued that the increased charge density and longer persistence length of dsDNA leads to larger DEP forces [6]. Here we postulate that the inherent differences between dsDNA and ssDNA, in addition to the difference in length of the dsDNA target and ssDNA probe, will allow for our devices to separate the two populations of DNA molecules.

3.0 DEP of DNA

3.1 Interdigitated Microelectrode Array

The first set of experiments was conducted using an interdigitated (IDT) microelectrode array, as shown in Figure 2a. This test setup is useful for preliminary experiments to determine the frequency-dependent DEP of a particular analyte. The multiple banks of microelectrodes promotes easy visualization of DEP, and the experimental setup is relatively simple (a drop of fluid containing the analytes is placed on the chip, and capped with a coverslip). The electrodes are bi-pronged, with each prong 5 μm wide separated by

a 5 μm space. Glass chips were prepared using a chrome mask to pattern photoresist into the inverse pattern of the microelectrode array. Ten nm of titanium, and then 100 nm of platinum were then evaporated on the chips. The resist was then removed with sonication in acetone, leaving the metal microelectrodes on the chip. The microelectrode features produce large field gradients ($\nabla E^2 \sim 10^{18}$ V^2/m^3, Fig. 2b), but the device does not have a microfluidic chamber to permit controlled fluid flow and analyte delivery. Large trapping forces are produced at the edges of the microelectrodes between prongs set to 5V and 0V, while minima in the gradient occurs in the centerline of each double-pronged microelectrode (blue region between the two 0 V prongs in Fig. 2b).

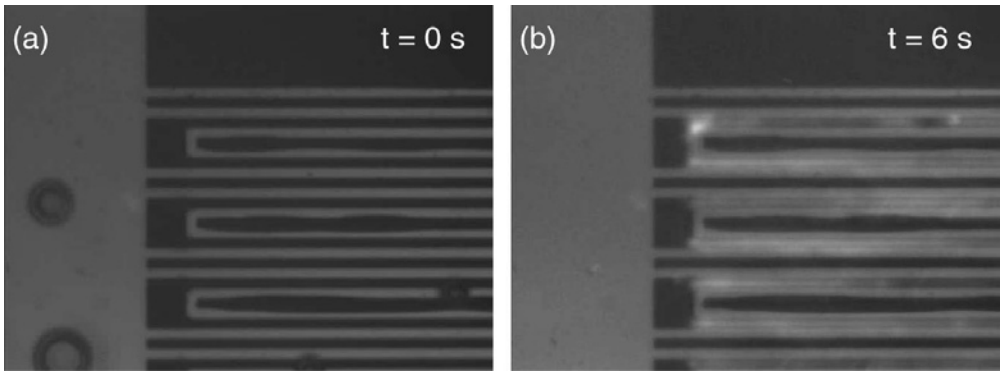

Figure 3: DEP trapping of DNA (1.1, 1.8, and 2.9 kbp) at 20 V p-p, 1MHz over a period of 6 seconds.

Experiments were conducted using samples from Columbia University. A DNA plasmid was digested (enzymes ScaI and HincII) to yield dsDNA strands of 1.1, 1.8, and 2.9 kbp. Twenty μL of a 220 ng/μL stock of the digested plasma in Tris-EDTA buffer was mixed with 10 μL of SYBR Green intercalating dye. The solution was then diluted to ~200 μL with DI water prior to application of 10-20 μL on a chip. Chips were placed beneath an upright fluorescence microscope with Rhodamine and Fluorescein filters. Chips were contacted with micrometer controlled probe tips, and actuated with a Protek 0-30 MHz frequency generator. The function generator was controlled manually, as well as with Sandia custom controller software (MEMScript). Video was monitored with an analog video camera and captured directly to the computer workstation with a National Instruments video capture card. Video was compressed and analyzed off-line.

There was evidence of DNA trapping in a span of frequencies from 100 kHz to 15 MHz. Strong quenching of the fluorescent dye occurred at 15 MHz, leading to rapid loss of signal. The cause of this effect is not known. Trapping at 100 kHz lead to significant competing effects to DEP, namely thermally-induced fluid flow as well as AC electroosmosis. Thus 1 MHz was chosen as the most appropriate frequency for trapping. Figure 3 shows rapid trapping of the DNA sample under a voltage of 20 V p-p at 1 MHz. The DNA is collected in regions between prongs that are set to 20 V and 0 V, with no trapping evident in regions between prongs set to the same voltage (either 0 or 20 V). This is expected from the plot of ∇E^2 in Figure 2, which indicates that the regions of largest gradient are located in these regions. The images show no evidence of strong

trapping at the edges of electrodes, but this may be partly due to quenching of the dye when the DNA is directly in contact with the electrode (a well-known phenomenon).

Figure 4a shows line-out plots of the fluorescence intensity from the experiment depicted in Figure 3. Line-outs are taken from the top to the bottom of each frame of the captured video. The first frame of each video was subtracted from subsequent frames to eliminate the background intensity of free DNA and the microelectrodes. In this instance, a line of length 120 µm containing five peaks (P1 to P5) of captured DNA was analyzed. Distances between peaks were approximately 20 µm, corresponding to the distance between opposed electrode prongs. Figure 4b shows the time course of DNA trapping at the five trap locations in (a). The average intensity value of peaks P1 to P5 was calculated for each time frame using ten values (five on each side) surrounding the maximum intensity of each peak. The average time course was fit with an exponential curve $A\text{-}Be^{-t/\tau}$, with A = -2.371, B = -0.105, and t = 1.75 s (r^2 = 0.981) [11]. Our time constant of 1.75 s was relatively short compared to the values obtained by Asbury, probably due to the smaller geometry of our microelectrodes.

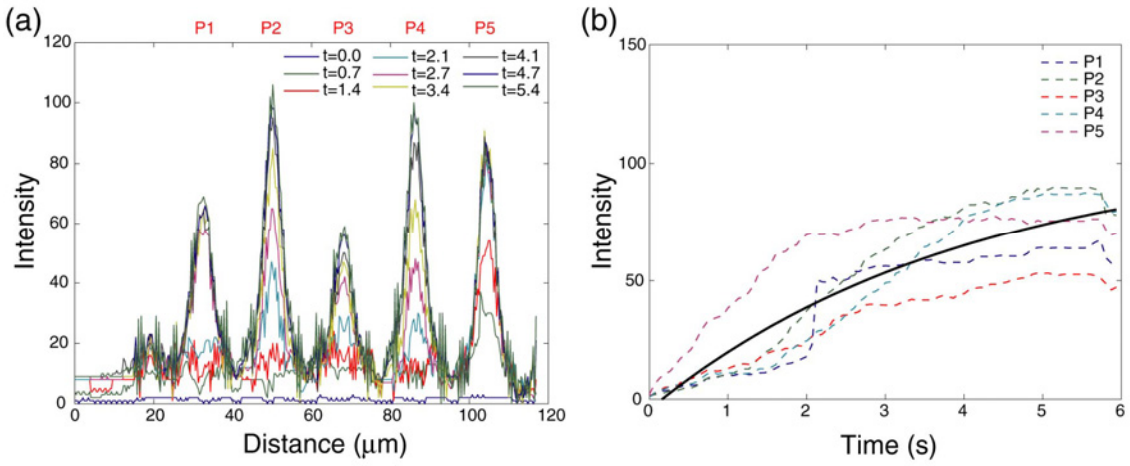

Figure 4: (a) Intensity plots of captured dsDNA on the IDT. Lineouts are taken from the video depicted in Figure 3 from t = 0 to t = 5.4 s. (b) Time course of DNA trapping at the five trap locations, P1 to P5.

A second set of experiments was conducted with a 60 bp ssDNA oligonucleotide supplied by our Columbia collaborators. Ten µL of SYBR Green and 10 µL of the oligonucleotide (100 µM in water) were combined and diluted to a total volume of ~200 µL with DI water. SYBR Green will bind to ssDNA, but at a much weaker binding strength than to dsDNA. This will present some difficulties with interpreting the data, but we intend to conduct further experiments to try to eliminate this problem. Figure 5 compares the capture of dsDNA to ssDNA in two separate experiments over similar time courses. The capture conditions were 20 V p-p at 1 MHz, and similar flow rates were observed although the ssDNA exhibited more aggregation than the dsDNA. The left plot depicts the fluorescence intensity lineouts of seven trap locations of dsDNA on the microelectrode device. Using a separate chip, an attempt was made to capture 60 bp ssDNA. The lineouts for ssDNA show no evidence of trapping in between oppositely

potentiated microelectrodes. In one experiment, the microelectrodes were set to 5V 1 MHz for twenty minutes (with the shutter closed) and still no trapping was observed. In

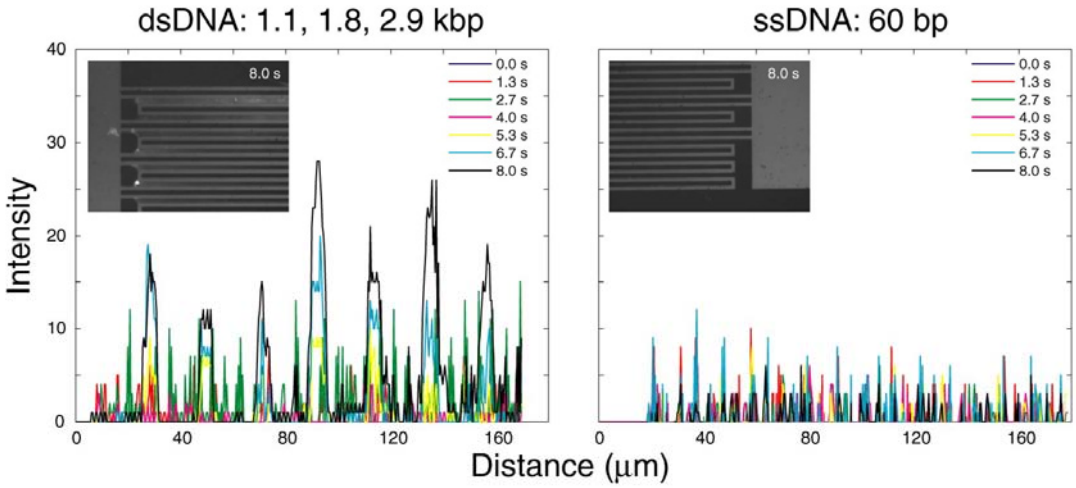

Figure 5: Capture of DNA under a DEP force (20 V p-p, 1 MHz). The dsDNA kbp sample shows significant capture (left), while the ssDNA 60 bp sample shows no significant capture (right). Insets are fluorescence images at t = 8s into the capture experiments.

several experiments, trapping of ssDNA aggregates (2-5 μm diameter globules) was observed. The data analyzed for dsDNA involved no DNA aggregates, and only included examples of capturing free-floating DNA. Further experiments, with more controlled DNA sample preparation, are required to determine the significance and effect of DNA aggregation on DEP capture. An advantage to the chip used in these experiments is the simple setup, and ease of use. A microfluidic device with flow channels for controlled delivery of fluid and analytes is the optimum setup for conducting more relevant experiments.

4.0 DEP Gating of DNA

4.1 DEP Gate Device

In conjunction with our colleagues from the New Jersey Institute of Technology, City College of New York, we have developed and demonstrated a new concept, termed "*dielectrophoretic gating,*" a technique that combines the field-induced dielectrophoresis and phase transition for manipulating particles in micro-fluidics [9,10]. Figure 1 depicts the gate, which consists of a pair of microelectrodes that span a fluid channel perpendicular to the direction of fluid flow. When an AC voltage is applied to the microelectrodes, an electric field is generated within the fluid channel. The range of the DEP force operating along the flow streamlines can be extended throughout the height (*z*-axis) of the channel by placing an electrode on the top and bottom surfaces of the channel. This helps to increase the gating efficiency in that analytes suspended in a fluid

flowing at any position in the *yz* plane will be subjected to the DEP force. The best technology for producing such a structure is the SwIFT^{TM} (Surface Micromachining with Integrated Fluidic Technology) process developed at Sandia [12]. The channels are fabricated in a fully encapsulated state, obviating the need for substrate bonding, a process that slows the device production and reduces reproducibility.

The devices were fabricated at the SNL Microelectronics Development Laboratory. SwIFT™ is a sacrificial layer method that uses multiple layers of structural materials (polysilicon and silicon nitride) and sacrificial materials (silicon oxide) to build devices. Up to five layers of fine-grained doped polysilicon (P0-P4) are used for making electrical connections and microelectrodes in order to impart electric fields into microfluidic compartments. Polysilicon layers are on the order of 1-2 μm thick, with the exception of P0, which is 0.3 μm. The structural layers of silicon nitride (N1: 0.3 μm, N2: 0.8 μm thick) provide optically transparent and electrically insulating surfaces that serve as bottom and top walls of the fluid channels. Figure 6b shows a close-up image of a completed device with 2 DEP gates. Etches are made in N1 and N2 to allow P0 and P3 electrodes to contact the fluid.

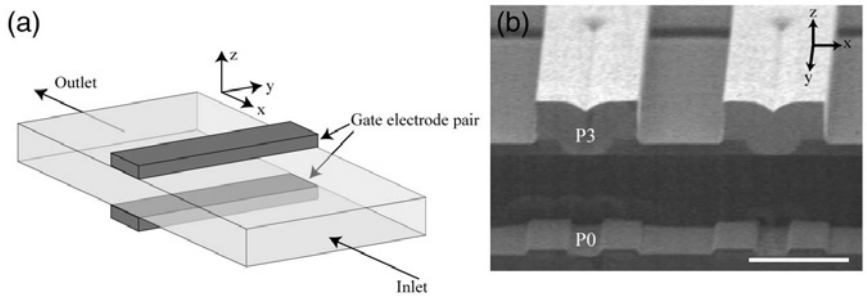

Figure 6: Schematic of a DEP gate consisting of two electrodes arranged perpendicular to the fluid flow in a channel (left). Cross-section of two micromachined DEP gates integrated with a microfluidic channel (right).

After completing the surface micromachining, access ports to the fluidic devices are fabricated using deep reactive ion etching [13]. The sacrificial oxide layers in devices are then removed in an HF-based etchant at 20^{o} C for 100-200 minutes depending on the length of the fluidic channel. The devices are then rinsed in deionized (DI) water and dried in supercritical CO_2. In preparation for experiments, capillaries (stainless steel and silica, outer diameter ~ 300 μm) are placed into the access ports and glued in place using high viscosity epoxy.

An advantage to the DEP gate is the electrodes on the top and bottom of the fluid channel. This allows the DEP force to be extended throughout the height of the fluid channel as depicted in the simulations in Figure 7. The gate is simulated for three conditions of the top (T) and bottom (B) gate electrodes: with T=B=10 V; T=10 V, B=0

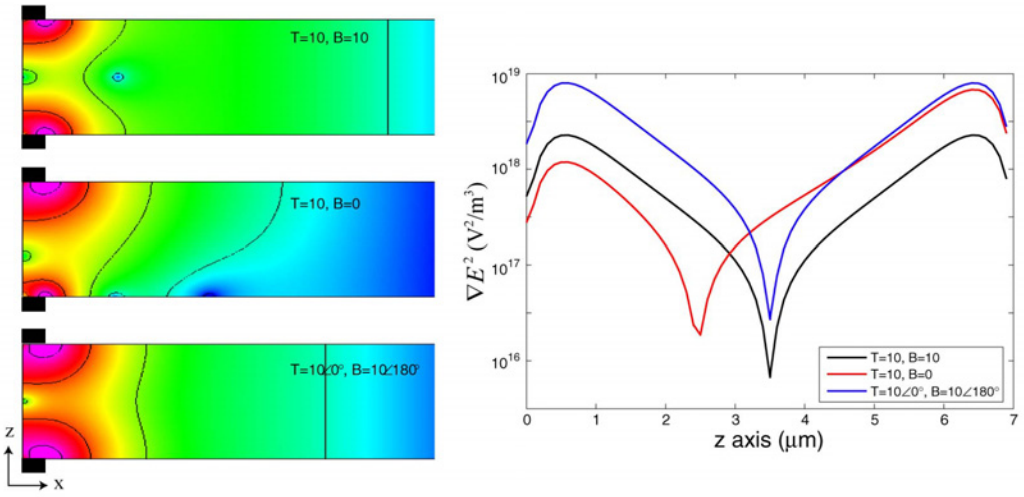

Figure 7: Simulation of $\nabla E^2(x,z)$ for three DEP gate conditions (left, pink= 10^{19} V^2/m^3 and blue = 10^{15} V^2/m^3). Electrodes (black rectangles) are added for clarity. Lineplots of $\nabla E^2(0,z)$ between the electrodes (right).

V; and T=10∠0°, B=10∠180°. Lineout plots of ∇E^2 along z between the two gate electrodes are also plotted. All three conditions produce large gradients near the electrodes, with minimums near the center of the channel as the distance from each electrode increases. The strongest trapping for pDEP will occur for the phased DEP gate condition, but the experimental setup requires two voltage sources that are phased. The other two conditions are the simplest to setup, with the 10 V/ 0 V (red curve) having a larger minimum (by approximately 3X), and thus better trapping efficiency.

4.2 DNA capture with a DEP Gate

DNA samples (1.1, 1.8, 2.9 kbp) were prepared and labeled with SYBR Green as detailed earlier. The DNA sample was loaded into teflon tubing by applying suction with a syringe. The teflon tubing was then fastened to stainless steel capillaries inserted into the access ports of the silicon microfluidic devices. Samples were injected into the device under manual pressure using a syringe.

The microdevice used is a 200 μm wide channel, 500 μm in length (Figure 8a). The DNA solution is entering through the access port shown on the right and the flowing to the left. The gate spanning the channel is located in the center of the channel, and the top electrode was set to 0 V, and the bottom electrode was set to 20 V p-p. Figure 8 depicts a DEP gate device held at 20 V p-p, 1 MHz. The gate was held at this voltage for approximately 1 minute, before being set to 0 V. Figure 8b shows lineplots of the fluorescence intensity at the dotted line (a). As performed previously, the first frame of the captured video was subtracted from subsequent frames to remove background fluorescence intensity from the free floating DNA and the microdevice. The black curves are the intensities before the trap is turned off. At t = 3.7 s, the gate is set to 0 V, and 70

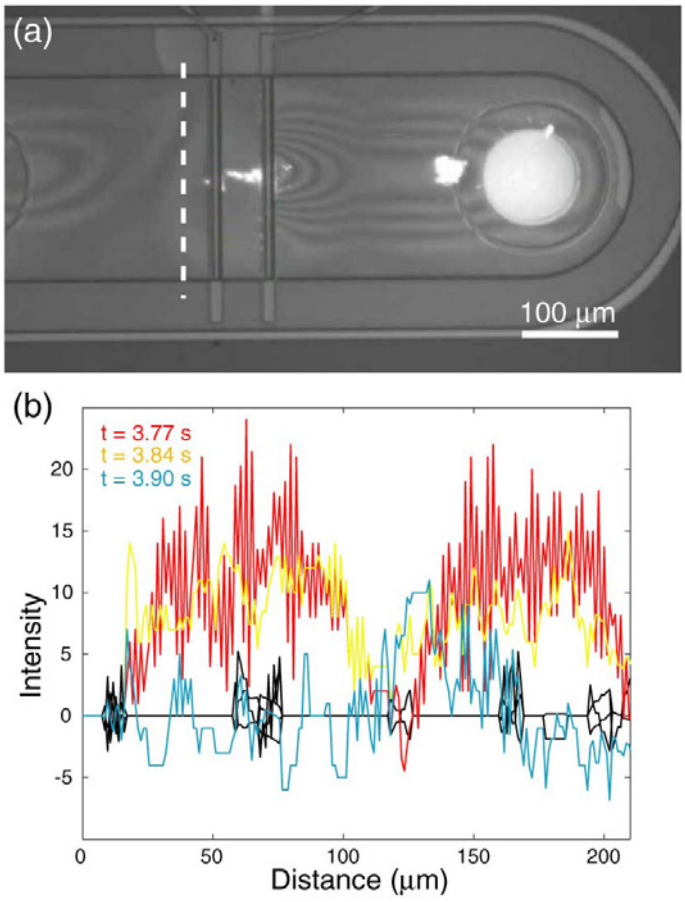

Figure 8: (a) A DNA sample is injected into a microfluidic channel with a DEP gate held at 20 V p-p, 1 MHz. Time is t = 3.70 s. (b) Lineplots of the fluorescence intensity (for each frame from t = 0 to 5 s, n=74 frames) at the dotted line located in (a). At ~3.70 s, the gate is set to 0 V. The black curves (n = 70 frames) are the background intensities and include the frames for t=0 to 3.70 s.

ms later we see a burst of fluorescence intensity as the band of captured DNA flows downstream. At t = 3.97s, the DNA band has completely traversed the observation point. The signal-to-noise ratio is relatively high after background subtraction (the DNA band shows up as a ~ 20% increase in background fluorescence before subtraction). The calculated velocity of the DNA band was approximately 1.5 mm/s initially, and slowing down to 0.3 mm/s as the band exits the channel. At an average fluid velocity of 0.3 mm/s, the flowrate through a single device is ~ 25 nL/min. Figure 9 shows a frame by frame depiction (background subtracted) of the released band of DNA. There is a slight non-uniformity in the shape of the DNA band, with large concentrations of DNA captured at the edges of the channel and a minimum in the captured DNA in the center of the channel.

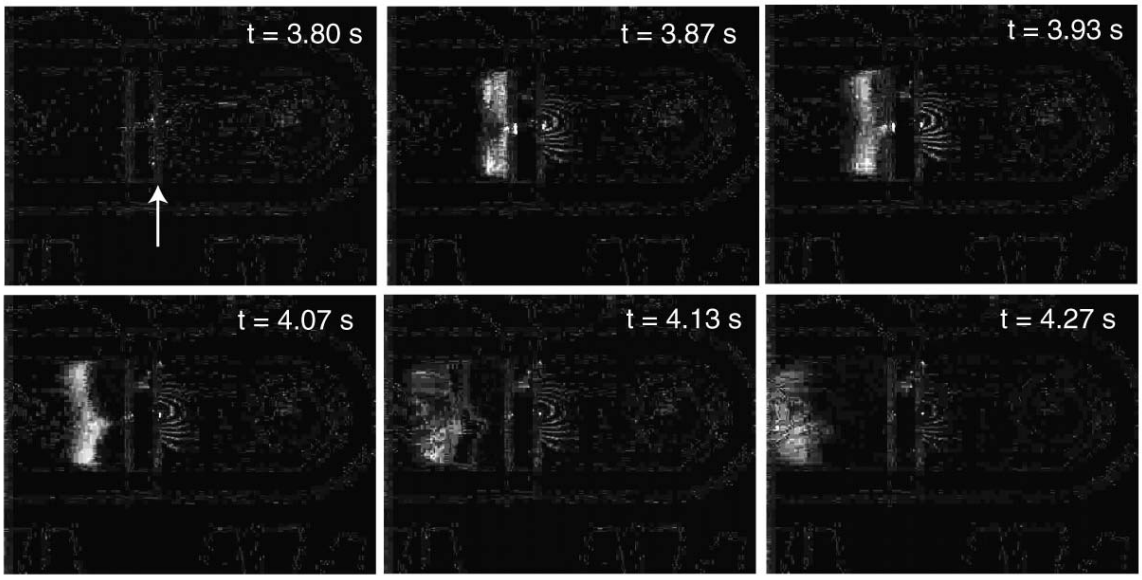

Figure 9: Release of preconcentrated dsDNA from a DEP gate (white arrow). The gate is set to 20 V p-p, 1 MHz. The voltage is set to 0 V at t = 3.70 s.

5.0 Discussion and Conclusions

This work has demonstrated the selective preconcentration of kilobase-pair double-stranded DNA (dsDNA). Using 20 V p-p 1 MHz voltages, we were able to preconcentrate dsDNA into pre-defined regions. Megahertz frequencies are well-suited for microdevices as they eliminate electrochemical effects (electroosmosis and water electrolysis), allowing larger voltage amplitudes to be applied. Trapping was fast (time constant of ~2 seconds) and depending on the device configuration, reversible. Small single-stranded oligonucleotides were not preconcentrated and can thus be flushed from a flow through system. Two different device configurations were used: an interdigitated electrode chip and a surface micromachined microfluidic flow-through device. The interdigitated electrode device contained a large number of traps, and in this device a considerable portion of the trap region exists in regions between microelectrodes. This promoted reversible trapping of dsDNA that released the DNA upon turning off the voltage. The flow-through microfluidic device contained only one trap, but the integrated fluid channel permits continued and controlled delivery of DNA to the trap region. A drawback to this device lies in the fact that the bulk of the trapping region is directly at the microelectrode edges, leading to some level of irreversible binding of trapped DNA to the electrodes. A combination of the design elements of each device would be optimum for high throughput reversible DNA preconcentration and binary large-target/small-probe separation.

Nucleic acid concentration factors can be estimated based on the fluid flow through the channel and the amount of material released as the channel is flushed. The degree of washing/cleaning (removal of non-trapped species of the nucleic acid can be roughly determined according to the dwell time used for trapping, the volume flow rate and the area of the channel:

$amount\ of\ DNA = \int_0^{t_t} ([DNA](vtA)dt)$ and the flush volume is $flush\ volume = \int_0^{t_f - t_t} ((vtA)dt)$ the relative concentration gain is then the amount of DNA divided by the flush volume or t_t/t_f for the case of constant flow rates and slow startup/valve time. Here *v* is the fluid velocity, A is the channel area, t_t is the time from start of flow till the channel is flushed, tf is the time converting from trapping to flushing, [DNA] is the concentration of nucleic acid in solution. The contaminants are however are reduced by the ratio of the volume of the DNA and the amount of impurity clinging to the sample and walls as compared to the flush volume. This can be a substantially higher number than the DNA concentration gain although it is difficult to estimate. Only after additional experimentation will we know if the relative amount of impurity is reduced enough to understand if the metrics for false positive rate reduction are met.

Several changes in the experiment will be pursued in order to clarify the operation of the technique. More experiments need to be conducted to ensure that ssDNA probes are being flushed from the system. In order experiments, it is possible that weak staining of the ssDNA lead to low capture results. And as mentioned previously, globular aggregates of ssDNA were observed to be collected under a DEP force. The effect of the sample preparation thus needs to be conducted to determine optimum conditions for preconcentrating kbp dsDNA and flushing ssDNA probes. A second consideration is to include anti-fading molecules (β-mercaptoethanol) to eliminate dye-quenching, an effect that was readily observed in most experiments.

As was mentioned above, the reality of adequately removing the unhybridized reporters must be ascertained in further work and will be the next step. Because of the relatively arbitrary amount of concentration and cleaning that can be performed simply by changing the flush times, we suspect that a series of cleanups and RT-PCR tests done in conjunction with Columbia will clarify the methodology to obtain clean readouts for new emerging pathogens.

6.0 References

1. Washizu, M., Suzuki, S., Kurosawa, O., Nishizaka, T., Shinohara, T., "Molecular dielectrophoresis of biopolymers," IEEE Transactions on Industry Applications 1994, Vol. 30, pg. 835.
2. F. Dewarrat, M. Calame, C. Schonenberger, "Orientation and positioning of DNA molecules with an electric field technique," Single Molecules 2002, 3, pp. 189-193.
3. C.L. Asbury, A.H. Diercks, G. van den Engh, "Trapping of DNA by dielectrophoresis," Electrophoresis 2002, 23, pp. 2658-2666.
4. Holzel, R., "Single particle characterization and manipulation by opposite field dielectrophoresis," Journal of Electrostatics 2002, Vol. 56, pg. 435.
5. Ying, L., White, S.S., Bruckbauer, A., Meadows, L., Korchev, Y.E., Klenerman, D., "Frequency and voltage dependence of the dielectrophoretic trapping of short lengths of DNA and dCTP in a nanopipette," Biophysical Journal 2004, Vol. 86, pg. 1018.
6. Chou C., Tegenfeldt, J.O., Bakajin, O., Chan, S.S., Cox, E. C., Darnton, N., Duke, T., Austin, R.H., "Electrodeless dielectrophoresis of single- and double- stranded DNA," Biophysical Journal 2002, Vol. 83, pg. 2170.
7. Wagner, K.W., Archive Electrotechnik 1914,Vol. 3, pg. 83.
8. Zheng, L., Brody, J.P., Burke, P.J., "Electronic manipulation of DNA, proteins, and nanoparticles for potential circuit assembly," Biosensors and Bioelectrronics 2004, Vol. 20, pg. 606.
9. Bennett, D.J., Khusid, B., James, C.D., Galambos, P.C., Okandan, M., Jacqmin, D., Acrivos, A., "Combined field-induced dielectrophoresis and phase separation for manipulating particles in microfluidics," Applied Physics Letters 2003, Vol. 83, pg. 4866.
10. James, C.D., Bennett, D.J., Okandan, M., Galambos, P.C., Khusid, B., Jacqmin, D., Acrivos, A., "Surface micromachined dielectrophoretic gates for the front-end device of a biodetection system," Journal of Fluids Engineering 2005, in press.
11. Asbury, C.L., van den Engh, G., "Trapping of DNA in nonuniform oscillating electric fields," Biophysical Journal 1998, Vol. 74, pg. 1024.
12. Okandan, M., Galambos, P.C., Mani, S., Jakubczak, J., "Development of Surface Micromachining Technologies for Microfluidics and BioMEMS," Proceedings of the SPIE International Society on Optical Engineering 2001, Vol. 4560, pg. 133.
13. Laermer, F., Schilp, A., 1996, "Method of anisotropically etching silicon," U.S. Patent Office, Pat No. 5,501,893.

Distribution:

5	MS1080	Conrad James	01769
1	MS1080	Paul Galambos	01769
1	MS1080	David Sandison	01769
3	MS1080	Mark Derzon	01769
1	MS0323	Donna Chavez	01011
1	MS9018	Central Technical File	8945-1
2	MS0899	Technical Library	9616